Research Article

Pulmonary Circulation

Hypercapnic acidosis attenuates pressure-dependent increase in whole-lung filtration coefficient (K_f)

Nikhil Bommakanti[1,2], Ayman Isbatan[1,3], Avni Bavishi[1,3], Gourisree Dharmavaram[1,3], Andreia Z. Chignalia[1,3] and Randal O. Dull[1,2,3]

[1]Department of Anesthesiology, University of Illinois at Chicago, College of Medicine, Chicago, IL, USA; [2]Department of Bioengineering, University of Illinois at Chicago, College of Medicine, Chicago, IL, USA; [3]Lung Vascular Biology Laboratory, University of Illinois at Chicago, College of Medicine, Chicago, IL, USA

Abstract

Hypercapnic acidosis (HCA) has beneficial effects in experimental models of lung injury by attenuating inflammation and decreasing pulmonary edema. However, HCA increases pulmonary vascular pressure that will increase fluid filtration and worsen edema development. To reconcile these disparate effects, we tested the hypothesis that HCA inhibits endothelial mechanotransduction and protects against pressure-dependent increases in the whole lung filtration coefficient (K_f). Isolated perfused rat lung preparation was used to measure whole lung filtration coefficient (K_f) at two levels of left atrial pressure ($P_{LA} = 7.5$ versus 15 cm H_2O) and at low tidal volume (LV_t) versus standard tidal volume (STV_t) ventilation. The ratio of K_{f2}/K_{f1} was used as the index of whole lung permeability. Double occlusion pressure, pulmonary artery pressure, pulmonary capillary pressures, and zonal characteristics (ZC) were measured to assess effects of HCA on hemodynamics and their relationship to K_{f2}/K_{f1}. An increase in P_{LA2} from 7.5 to 15 cm H_2O resulted in a 4.9-fold increase in K_{f2}/K_{f1} during LV_t and a 4.8-fold increase during STV_t. During LV_t, HCA reduced K_{f2}/K_{f1} by 2.7-fold and reduced STV_t K_{f2}/K_{f1} by 5.2-fold. Analysis of pulmonary hemodynamics revealed no significant differences in filtration forces in response to HCA. HCA interferes with lung vascular mechanotransduction and prevents pressure-dependent increases in whole lung filtration coefficient. These results contribute to a further understanding of the lung protective effects of HCA.

Keywords

hypercapnic acidosis, pulmonary edema, filtration coefficient, mechanotransduction, rat

Date received: 16 March 2017; accepted: 13 July 2017

Pulmonary Circulation 2017; 7(3) 719–726
DOI: 10.1177/2045893217724414

Background

Low tidal volume ventilation has been shown to improve survival in acute respiratory distress syndrome (ARDS)[1] and is a key component of lung-protective ventilatory strategies. The concomitant increase in CO_2 accumulation leads to hypercapnic acidosis (HCA), which has both beneficial and harmful effects depending on the disease state, e.g. attenuating pulmonary edema in mechanical models of lung injury but inhibiting neutrophil function and worsening outcomes in infectious models of lung injury.[2,3] HCA has been studied extensively in non-septic models of mechanical lung injury where high-tidal volume ventilation has been used to induce ventilator-induced lung injury (VILI). A principle mechanism to account for the protective effects of HCA in VILI is the inhibition of NF-kB,[4] a key regulatory protein in many inflammatory pathways. HCA also attenuates the inflammatory activation of p42/44 MAP-kinase, an enzyme that has numerous effects on cytoskeletal and focal adhesion proteins that are directly involved in endothelial permeability.[5,6] We have shown that airway pressure is synergistic with vascular pressure in altering K_f;[7] thus, the ability of HCA to mitigate alveolar injury during VILI prompted us to hypothesize that HCA

Corresponding author:
Randal O. Dull, Department of Anesthesiology, 1740 West Taylor Street, Suite 3200, Chicago, IL 60612, USA.
Email: rdull@uic.edu

may also influence endothelial barrier function during mechanical stress.

The acute increase in P_aCO_2 and resulting decrease in pH have effects on pulmonary hemodynamics that are complex and dependent upon pre-existing vascular tone. In general, HCA increases pulmonary artery pressure (PAP)[8,9] by vasoconstriction of both pre- and post-capillary vessels[10] and stimulates sympathetic activity as evidenced by increases in plasma epinephrine and norepinephrine concentrations.[11] Collectively, these responses increase heart rate, mean pulmonary arterial pressure (mPAP), and mean pulmonary capillary pressure (P_{Pc}). Thus, we found it curious that HCA could reduce pulmonary edema in models of lung injury when vascular permeability and hydrostatic pressures were both increased. While HCA may attenuate increases in endothelial permeability induced by inflammatory pathways, the elevated hydrostatic pressure would increase fluid filtration and, therefore, increase edema. One might expect, therefore, that increased filtration induced by elevated hydrostatic pressure would nullify the anti-inflammatory effect(s) of HCA on edema development.

In addition to the simple increase in filtration pressure that promotes edema development, increased hydrostatic pressure activates endothelial mechanotransduction and leads to enhanced endothelial permeability. For example, Czarny and Schnitzer demonstrated that increased pressure and flow activated neutral sphingomyelinase, resulting in the release of ceramide, a potent activator of endothelial nitric oxide synthase.[12,13] As we have previously reported, pressure-dependent nitric oxide production is associated with increased endothelial permeability and acute barrier failure as assessed by the whole lung filtration coefficient[7] and an increase in hydraulic conductivity of lung microvascular endothelial cells.[14] To explain the beneficial effects of HCA on reducing pulmonary edema during experimental lung injury, we tested the hypothesis that HCA inhibits pressure-induced endothelial mechanotransduction.[7]

Methods

Isolated perfused lung preparation (IPL)

All animal experiments were approved by the University of Illinois at Chicago Animal Care Committee, and were conducted in accordance with the Guide for the Care and Use of Laboratory Animals (National Research Council). Adult male Sprague-Dawley rats (300–400 g) were anesthetized with ketamine/xylazine (90/10 mg/kg). A tracheotomy was performed and the animals were mechanically ventilated with a pressure-controlled ventilator (Kent Scientific, Torrington, CT, USA) at a respiratory rate of 60/min. Low tidal volume (L_{Vt}) ventilation with low peak inspiratory pressure (PIP = 6–8 cm H_2O) was compared with standard tidal volume (ST_{vt}) ventilation with standard peak inspiratory pressure (PIP = 10–13 cm H_2O) as described previously.[7] Following sternotomy, the pericardial sac was opened, ligatures were placed around the aorta and pulmonary artery, and heparin (200U) was injected into the right ventricle and allowed to circulate for 2 min. The left atrium was cannulated via a small incision in the left ventricle and the pulmonary artery was cannulated via the right ventricle; lungs were perfused with Krebs-Ringers bicarbonate solution (Sigma Chemical, St. Louis, MO, USA) containing 3% bovine serum albumin (BSA; Fraction V; Proliant, Ankeny, IA, USA).

PAP and left atrial pressures (P_{LA}) were measured continuously via in-line pressure transducers (P-75, Harvard Apparatus, Natick, MA, USA) connected to an A/D board (NI-DAQ USB-6211 National Instruments, Austin, TX, USA). In-line solenoid valves (20PSI, 12V DC, Cole Parmer, Mount Vernon, IL, USA) on both the arterial and venous tubing could be closed simultaneously for measuring double occlusion pressures (P_{DO}). An in-line ultrasonic flow probe (Harvard Apparatus, Natick, MA, USA) on the pulmonary artery cannula recorded flow data in real time. The perfusion rate was 6 mL/min. Lungs were excised and suspended from a force transducer (Radnoti, Minrovia, CA, USA) and lung weight was continuously measured. Lung weight, vascular pressures, and flow were recorded using a custom-written program (LabVIEW 8.2, National Instruments, Austin, TX, USA).

Pressure–volume relationship

Tidal volumes (V_t) in isolated perfused rat lungs during pressure-controlled ventilation were measured as previously described.[7] Briefly, a differential pressure transducer (DP-45, Validyne, Northridge, CA, USA), driven by a carrier frequency bridge amplifier (Type 677, Hugo Sachs Elektronik-Harvard Apparatus) was used to record airflow (mL/s) at a sampling rate of 200 Hz using a custom-written program (LabVIEW 8.5, National Instruments, Austin, TX, USA). Each respiratory cycle was integrated to obtain V_t. A calibration curve was created by applying airflow (air pressure = 1 bar) from negative 16.16 mL/s (vacuum) to positive flow at 16.16 mL/s, through the DP-45 and recording the corresponding voltage output. Flow was regulated with a calibrated flowmeter (Dwyer, model UA1049; accuracy ± 2%) connected to a pressure regulator. The lungs were ventilated with a range of PIPs and positive end-expiratory pressures (PEEPs) to record the resulting V_T values. Flow/V_t was recorded for 1 min for each ΔP (ΔP = PIP–PEEP). We used inflation pressures that produced V_T identical to previous literature values[15,16] during standard tidal volume (STV_t). Low tidal volume ventilation (Low V_t) inflation pressures were chosen to mimic clinically relevant lung-protective strategies. Lung-protective ventilation strategies are typically described in mL/kg; thus, despite using a pressure-controlled ventilator, we present the results as Low V_t and Standard V_t based on the pressure-volume relationship in Fig. 1a.

The pressure–volume curve presents ΔP (PIP–PEEP) versus V_t (normalized to body weight [kg]) (Fig. 1a). The

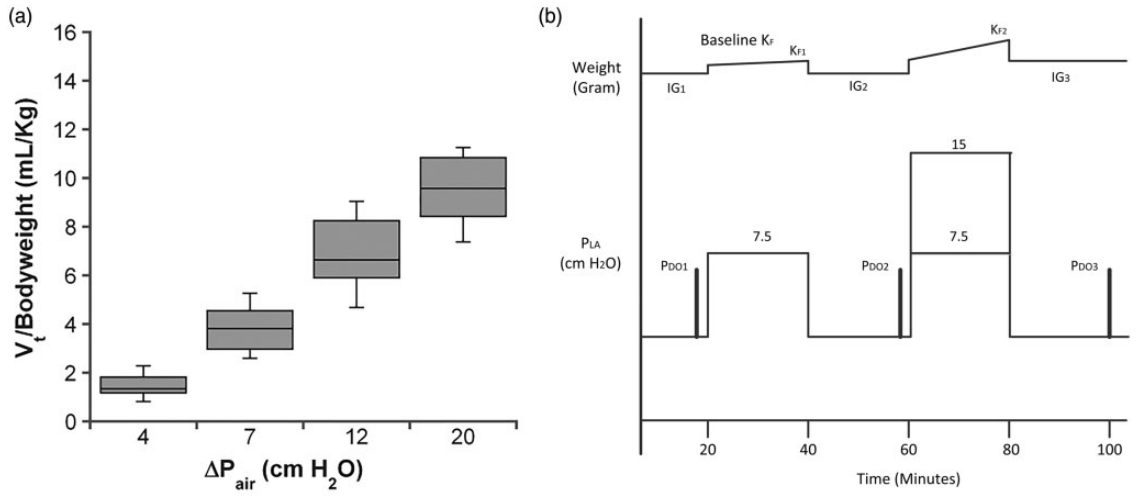

Fig. 1. (a) Pressure–volume (P-V) relationship: P-V relationship for ventilation strategies used for low tidal volume group and standard tidal volume group. See "Methods" for details. (b) Experimental protocol. Isolated perfused lungs were suspended from a force transducer and real-time changes in weight were recorded (g) as a function of left atrial pressure (P_{LA}, cm H_2O). Isogravimetric (IG) conditions were achieved at basal PLA (2 cm H_2O). Double occlusion pressures (P_{DO}) were performed before each increase in P_{LA} and at the end of the experiment. Whole lung filtration coefficient (K_f) was measured at $P_{LA} = 7.5$ cm H_2O and taken to be baseline; K_f was then measured after Step 2 ($P_{LA} = 15$ cm H_2O); the ratio of K_{f2}/K_{f1} was used to derive change in whole lung permeability.

low V_t group was ventilated with 6–8 cm H_2O providing a V_t per body weight of approximately 3–5 mL/kg. The ST V_t group was ventilated with 10–12 cmH_2O yielding V_t per body weight of 6–8 mL/kg.

Calculation of K_f

The rate of change in lung weight (g) between 18–20 min of the left atrial pressure step was divided by P_{Pc}, where $P_{Pc} = (PAP + P_{LA})/2$, to yield mL/min/cm H_2O (17). This value was normalized to 100 g of predicted lung weight (PLW) using the equation, PLW = 0.0053* (rat weight) – 0.48.

Zonal characteristic (ZC)

K_f measurements are dependent on vascular surface area available for fluid filtration and differences in vascular recruitment can result in spurious increases in K_f. To determine if HCA altered vascular recruitment, ZCs, i.e. percentage of West Zone 2 and 3 conditions were derived for each test group. ZCs were calculated according to $ZC = \Delta PAP/\Delta P_{LA}$ as described in the references.[18,19]

Experimental protocols

Protocol 1. LV_t: Isolated perfused lungs were ventilated at L_{Vt} and kept at isogravimetric pressure for 20 min. The P_{LA} was then increased to 7.5 cmH_2O for 20 min. After a second 20-min isogravimetric period, the lungs were again subjected to a P_{LA} step of 7.5 cmH_2O (Group C), 15 cmH_2O (Group P), or 15 cmH_2O + HCA (Group P+HCA). Finally, the lungs were returned to a third isogravimetric condition for 20 min (Fig. 1b). K_{f1} was derived during the first P_{LA} step; K_{f2} was derived during the second pressure step; PAP and P_{LA} were measured during both pressure steps, and P_{DO}s were measured after each pressure step.

Protocol 2. STV_t: Isolated, perfused lungs were ventilated with STV_t and subjected to two left atrial pressure steps and three isogravimetric periods as described above. The second left atrial pressure step was 7.5 cmH_2O (Group C), 15 cmH_2O (Group P), and 15 cmH_2O with HCA (Group P+HCA).

Hypercapnic acidosis. HCA was achieved by bubbling CO_2 into the perfusate reservoir to establish a pH of 7.10–7.15 that equates to a P_{CO2} of approximately 65–70 mmHg. pH was monitored throughout the experiment and CO_2 infusion rate was adjusted to maintain appropriate pH. Lungs were exposed to HCA starting 10 min into the second isogravimetric period and continuing through the second increase in left atrial pressure. Total time for exposure to HCA was 30 min.

Neutral sphingomyelinase. Neutral sphingomyelinase was inhibited by adding 20 μM GW4869 to the perfusate 10 min into the second isogravimetric period. GW was only tested using STV_t at 15 cm H_2O (Group P+GW).

Statistics

Data are presented as box plots showing median and interquartile range (IQR) as well as whiskers drawn to the most extreme values that fall within 1.5 times the IQR. Groups were compared using the Kruskal–Wallis rank sum test

followed by Dunn's test using R 3.3.1 with the data.table, dunn.test, ggplot2, and cowplot packages.[20–24] Significant difference between groups was determined at $P < 0.05$.

Results

Hemodynamics

All lungs were exposed to a $P_{LA} = 7.5$ cm H_2O to determine baseline hemodynamic variables and baseline K_f, before exposure to either high P_{LA} (Group P: $P_{LA} = 15$ cm H_2O) or high P_{LA} + HCA and are presented in Fig. 2. In the L_{Vt} group, PAP was slightly higher (by 1.5 cm H_2O) in P versus P+HCA ($P = 0.042$) while there were no differences in P_{pa} during ST_{Vt} conditions.

During LV_t, P_{Pc} was slightly increased from 17.50 to 18.30 cm H_2O ($P = 0.011$) but during STV_t no differences existed ($P = 0.38$). The P_{DO} for LV_t Group P+HCA versus Group P was 3.4 versus 4.5 cm H_2O ($P = 0.003$); during STV_t there was no difference in P_{Do} between Group P versus Group P+HCA ($P = 0.432$).

Zonal characteristics

To rule out pH-dependent changes on vascular tone, recruitment, and vascular surface area that could affect measurement of K_f, ZC was derived as an indicator of zone II and zone III conditions. During L_{Vt}, increasing P_{LA2} from 7.5 cm H_2O to 15 cm H_2O (Group C versus Group P) resulted in an increase in ZC to 0.76 ± 0.061 from 0.59 ± 0.066 ($P = 2.0e\text{-}04$). Group P + HCA had no effect on ZC compared with Group P (Group P+HCA 0.73 ± 0.044 versus Group P 0.76 ± 0.061; $P = 0.44$) (Fig. 2, left column).

During STV_t, increasing P_{LA2} from 7.5 cm H_2O to 15 cm H_2O increased ZC to 0.78 ± 0.074 from 0.45 ± 0.044 ($P = 2.3e\text{-}03$). Group P + HCA had no effect on ZC compared with Group P (Group P+HCA 0.80 ± 0.053 versus Group P 0.77 ± 0.074, $P = 0.23$) (Fig. 2, right column). The absence of any differences in ZC between Group P versus Group P + HCA indicates that changes in vascular recruitment and surface area were not responsible for the observed differences in K_f.

Baseline K_f

Each preparation was subjected to an initial pressure step in P_{LA} to 7.5 cmH_2O for 20 min. The K_f measured during the initial pressure step was termed K_{f1}. Each K_{f1} served as an individual control to account for the natural variation in baseline permeability between isolated lung preparations; filtration is reported as K_f during the second pressure step, K_{f2}, normalized to K_{f1} (K_{f2}/K_{f1}). K_{f1} was compared across experimental groups to ensure any differences observed in K_{f2}/K_{f1} could not be attributed to differences in starting conditions. There was no difference in K_{f1} across groups at Lv_t ($P = 0.053$) or STV_t ($P = 0.19$; Fig. 3).

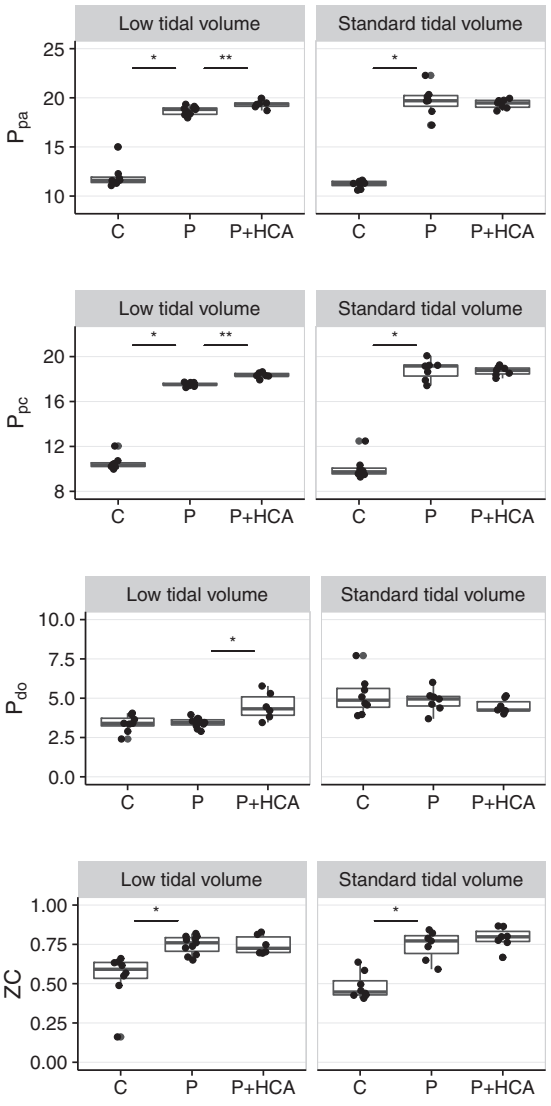

Fig. 2. Effect of HCA on pulmonary hemodynamic variables. Left column: hemodynamic variables for low tidal volume group. PAP and P_{Pc} increased significantly between C vs. P (*$P = 0.0014$). P_{Pa} increased slightly in P + HCA vs. P (**$P = 0.042$); P_{Pc} was significantly increased during HCA vs. P (**$P = 0.011$). P_{DO} was significantly higher in P + HCA vs. P (*$P = 0.003$). ZC was significantly increased in C vs. P. No differences in ZC were observed between P vs. P+HCA. Right column: hemodynamic variables for STV_t group. PAP and P_{Pc} were higher in P vs. C ($P = 0.0002$ and 0.003, respectively). There were no differences in PAP, P_{Pc}, P_{DO}, or ZC for P vs. P + HCA.

Increased P_{LA} and K_{f2}/K_{f1}

To characterize the influence of increased vascular pressure on K_f, lungs were exposed to a second step increase in P_{LA2} to 15 cmH_2O for 20 min (Group P). During LV_t, increasing P_{LA2} to 15 cm H_2O (n = 11) increased K_{f2} to 0.14 ± 0.047 from $0.049 + 0.016$ mL/min/cmH_2O per 100 g wet lung weight and resulted in a K_{f2}/K_{f1} of 3.4 ± 1.8, a 4.9-fold increase compared to the K_{f2}/K_{f1} of 0.69 ± 0.38 for Group C (n = 8) where P_{LA2} was set to 7.5 cmH_2O for 20 min ($P = 2.9e\text{-}5$; Fig. 4).

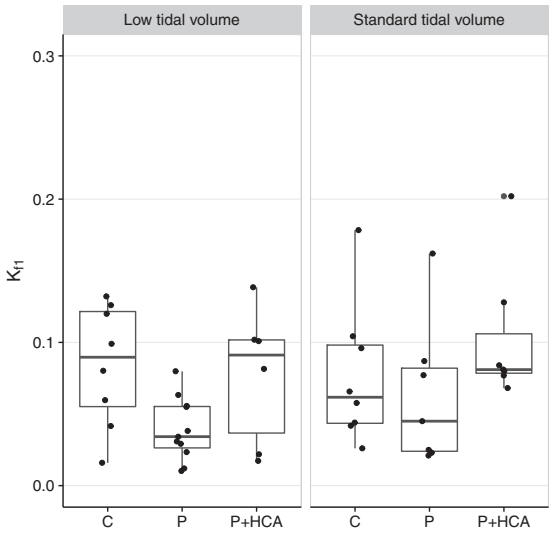

Fig. 3. Baseline K_{f1} across groups. All groups had K_{f1} measured at PLA = 7.5 cm H_2O to assess baseline conditions. K_{f1} for all groups during both LV_t and STV_t are statistically similar indicating that baseline K_f did not affect final K_{f2}/K_{f1}.

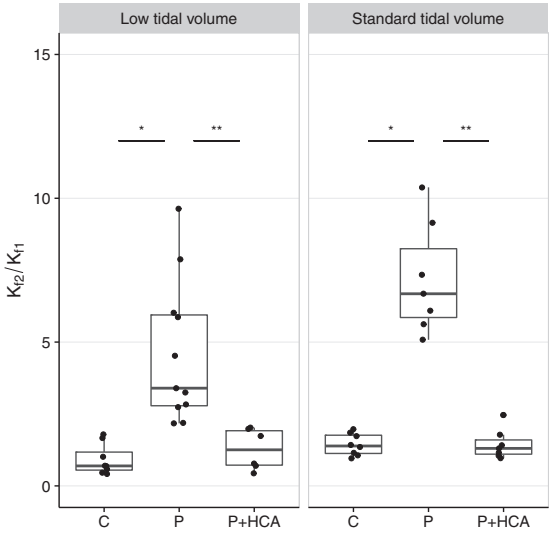

Fig. 4. Effect of HCA on K_{f2}/K_{f1}. K_{f2}/K_{f1} was derived during control conditions (Group C) vs. high pressure (Group P) vs. high Pressure + HCA (Group P + HCA) during both LV_t (left) and STV_t (right). In the LV_t group, K_{f2}/K_{f1} increased 3.4 (C vs. P). When HCA was induced prior to PLA = 15 cm H_2O (Group P + HCA), K_{f2}/K_{f1} was maintained at baseline values; *Group P > Group C, $P = 2.9e\text{-}05$; **Group P > Group P + HCA, $P = 1.9e\text{-}03$. During STV_t, K_{f2}/K_{f1} increased by 4.9-fold between Group C vs. Group P. HCA prevented increase in K_{f2}/K_{f1} during high pressure (Group P+HCA): *Group P > Group C, $P = 1.3e\text{-}03$; **Group P > Group P + HCA, $P = 5.8e\text{-}03$.

During STV_t, increasing P_{LA2} to 15 cm H_2O (Group P; n = 7) increased K_{f2} to 0.41 ± 0.39 from 0.082 ± 0.038 mL/min/cmH_2O per 100 g wet lung weight ($P = 1.3e\text{-}3$) and resulted in a K_{f2}/K_{f1} of 6.7 ± 1.6, a 4.8-fold increase

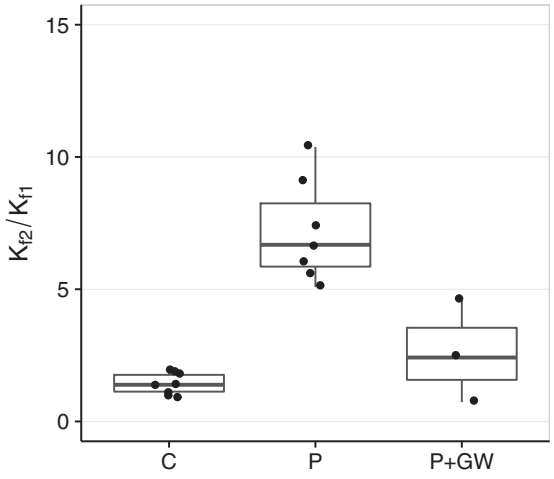

Fig. 5. Neutral sphingomyelinase inhibition attenuates pressure-mediated increase in K_{f2}/K_{f1}. Rat lung K_f was derived during control conditions (Group C, PLA = 7 cm H_2O) and after a step increase to PLA = 15 cm H_2O (Group P) during STV_t conditions. K_{f2}/K_{f1} was significantly increased in Group P vs. Group C (*$P = 0.014$) but was significantly attenuated by inhibition of neutral sphingomyelinase (Group P + GW, **$P = 0.014$). Thus, inhibition of neutral sphingomyelinase prevents pressure-dependent increase in at lung K_f.

compared with the Group C (n = 8) K_{f2}/K_{f1} of 1.4 ± 0.50 ($P = 6.9e\text{-}4$; Fig. 4).

Hypercapnic acidosis

HCA eliminated the effects of increased P_{LA} on K_{f2}/K_{f1} in the L_{Vt} group (n = 6). At LV_t, HCA reduced K_{f2} to 0.089 ± 0.097 from 0.14 ± 0.047 mL/min/cm H_2O per 100 g wet lung weight (Group P + HCA versus Group P, $P = 0.067$), resulting in a K_{f2}/K_{f1} of 1.25 ± 0.95. This value was significantly different from group P ($K_{f2}/K_{f1} = 3.4 \pm 1.8$; $P = 1.9e\text{-}3$) but not significantly different from Group C ($K_{f2}/K_{f1} = 0.70 \pm 0.38$; p = 0.23; Fig. 4), indicating a return to baseline permeability.

At STV_t, HCA reduced K_{f2} to 0.12 ± 0.042 from 0.41 ± 0.39 mL/min/cm H_2O per 100 g wet lung weight (Group P + HCA versus Group P, $P = 0.038$) and returned the K_{f2}/K_{f1} ratio to 1.3 ± 0.38 (versus Group P, $P = 5.8e\text{-}4$; versus Group C, $P = 0.44$; Fig. 4).

Neutral sphingomyelinase inhibition

GW4869, a neutral sphingomyelinase inhibitor, was tested at $P_{LA2} = 15$ cmH_2O in the STv_t group (n = 3). GW4869 administration during $P_{LA2} = 15$ cmH_2O reduced K_{f2} to 0.24 ± 0.16 from 0.41 ± 0.36 mL/min/cm H_2O per 100 g wet lung weight (versus Group P; $P = 0.014$), resulting in a K_{f2}/K_{f1} of 2.4 ± 2.5. This was significantly different from the Group P ($P = 0.014$) and not significantly different from Group C (K_{f2}/K_{f1} of 1.4 ± 0.50; $P = 0.29$; Fig. 5).

Discussion

We investigated the effect of HCA on K_f using the isolated perfused rat lung model and investigated the hemodynamic consequences of HCA on pressure-dependent endothelial barrier function. The major findings of the present study are that HCA, within a clinically acceptable range (pH 7.10–7.15): (1) inhibited pressure-induced increase in the whole lung filtration coefficient (K_f) at both low tidal volume ventilation and standard tidal volume ventilation; (2) had minimal effects on PAP and P_{Pc}; and (3) had no effect on ZCs that could explain the change in K_f. In addition, we demonstrate that inhibition of neutral sphingomyelinase attenuates pressure-dependent changes in K_f during STV_t. Collectively, these data suggest that HCA enhances barrier function in lung vascular endothelium by attenuating pressure-dependent mechanotransduction.

In our analysis of HCA on K_f, it is important to distinguish the direct versus indirect effects of HCA on the pulmonary vascular pressure. In an intact animal, HCA increases pulmonary vasculature pressures by activating sympathetically mediated reflexes[8,11] that shift blood volume from the splanchnic circulation to the pulmonary circulation.[25] The lung vasculature is a low-compliance system, possessing only one-seventh the compliance of the overall systemic circulation,[26,27] meaning that small changes in blood volume distribution create large changes in hydrostatic pressure. In the isolated perfused rat lung preparation, HCA caused minor vasoconstriction leading to a small increase in PAP, presumably via actions on both pre- and post-capillary vessels.[9,10] An increase in pre-capillary resistance would protect the downstream exchange vasculature from elevated pressures and reduce K_f, while an increase in post-capillary resistance would increase capillary pressure and increase K_f. An increase in both pre- and post-capillary resistances would likely offset each other resulting in no change in K_f. We measured PAP, P_{Pc}, and P_{DO} after HCA exposure and noted a small (1–2 cm H_2O) increase in both PAP, P_{Pc}, and P_{DO} (Fig. 2). These increases in pressure during HCA should have increased K_f and not reduce K_f as we observed. Thus, changes in hydrostatic pressure and ZC cannot explain the effect of HCA on K_f.

In the lung vasculature, hydrostatic pressure-dependent mechanotransduction involves several known effector proteins including: heparan sulfate proteoglycans;[7] nitric oxide synthase;[7,14] TRPV4;[28] neutral sphingomyelinase;[12,13] and PECAM.[29] Despite this list of known entities, a unifying model for pressure-sensing and coordinated downstream signaling that modulates permeability has yet to be validated. The influence of hydrostatic pressure on endothelial permeability via heparan sulfate-[7,14] and TRPV4-[28] dependent changes on lung permeability has been described in detail and both likely involve downstream activation of NOS. Increased concentration of intra-cellular nitric oxide is associated with nitrosylation of adherens junction proteins and subsequent disassembly of the adherens junction leading to increased permeability.[30–32]

Czarny et al.[13] were the first to demonstrate that lung endothelial membrane fractions isolated after exposure to increased pressure or flow exhibited increased neutral sphingomyelinase (N-SMase) activity. Follow-up studies by Czarny et al.[12] reported that inhibition of N-SMase prevents lung vascular mechanotransduction via a reduction in endogenous ceramides, while exogenous ceramide mimics the effects of mechanotransduction. High pressure- and flow-induced ceramide release and exogenous ceramide stimulated the phosphorylation of MEK1/2, AKT, eNOS(ser1177) and Src-like kinases. This work, however, did not demonstrate a direct link between changes in neutral sphingomyelinase activity and changes in permeability. The inhibition of N-SMase with GW4869 and the attendant protective effect on pressure-induced whole lung permeability represents direct evidence for the role of N-SMase in lung vascular barrier regulation. Activated N-SMase rapidly generates ceramide, a director activator of Enos;[33,34] thus, it seems highly likely that heparan sulfate proteoglycans, directly or indirectly, activate N-SMAse to release ceramide which in turn activates eNOS. As we have shown in endothelial monolayer studies and the isolated perfused lung preparation, increased NO production is associated with an increase in endothelial permeability by promoting adherens junction disassembly.

Acute increases in hemodynamic forces, either by pressure or flow, stimulate the disassembly of the adherens junction, resulting in increased permeability. Activation of nitric oxide synthase is an ubiquitous response to increases in pressure and shear stress, having been demonstrated in HUVECs,[35] BLMVEC,[14] BAEC,[36] and rat mesenteric vessels in vivo.[37,38] For example, DeMaio et al.[39] demonstrated that an acute increase in hydrostatic pressure (from 0 to 10 cm H_2O) was associated with a biphasic response by junctional proteins. Initially, ZO-1 was observed to undergo translocation from the cytoplasm to the adherence junction where it contributed to the ''sealing response,'' whereby cells adapt to the sudden increase in pressure by creating tighter junctions. However, further increases in hydrostatic pressure activates secondary mechanosensitive signals that stimulate NOS activation, NO production, and junctional disassembly leading to increased hydraulic conductivity and increased K_f in monolayers and whole lungs, respectively.[7,14,36] eNOS-dependent nitration of p190RhoGap-A is a principle mechanism for adherence junction disassembly.[30] In addition, oxidant signaling induces the interaction $G_{\alpha 13}$ with VE-cadherin at the p120-catenin binding site leading to VE-cadherin removal, internalization, and degradation resulting in hyperpermeability.[32]

Despite the aforementioned discussion of our interpretation of the current data and the extensive literature citations that support the idea of a pressure-eNOS mechanism that regulates barrier function, one publication has reported that NO preserves barrier function during elevated hydrostatic pressure. Yin et al.[40] reported that inhibition of eNOS using LNAME increased rat lung K_f and resulted in worse

edema formation. We have reviewed the difference in experimental approach of Yin et al. in our paper and Dull et al.[7] Briefly, a major difference that may explain the results of Yin et al. is the role of cyclic ventilation in maintaining endothelial cGMP levels. Yin et al. used a model where the lungs were held in a statically inflated state and not subjected to cyclic mechanical ventilation. Lung cGMP levels are positively influenced by mechanical ventilation and non-ventilated lungs show a significant reduction in cGMP levels.[41–43] Kuebler,[44] in "*The Janus-faced regulation of endothelial permeability by cGMP*," reviewed the disparate effects of cGMP on endothelial barrier function, where cGMP can be either barrier-protection or barrier-disruptive. As Kuebler presented in this review, intra-cellular concentrations of cyclic nucleotides, the ratios of cGMP/cAMP, sub-cellular compartmentalization of cyclic nucleotides, and the activities of PDE2A and PDE3, will determine the ultimate effects of cGMP on endothelial barrier properties and K_f. We assume that the use of cyclic ventilation in our model and the prevailing hemodynamic forces within the pulmonary endothelium maintained cyclic nucleotide concentrations such that NO produced barrier-disrupting processes.

Clinical relevance

Lung vascular mechanotransduction is most likely to be operational during states of acute heart failure (HF) where pulmonary vascular pressure increases rapidly. This can occur as a result of left ventricular dysfunction or sympathetically induced blood volume shifts from the periphery to the central compartment. The hemodynamic changes required to activate mechanotransduction and lead to barrier failure are quite modest. An increase in P_{Pc} of 8 cmH_2O for 20 min resulted in a fivefold increase in K_f[7], while Kuebler et al.[45] showed that an increase in $\Delta P_{LA} = 10$ cm H_2O resulted in a 4.6-fold increase in lung NO-dependent fluorescence.

Limitations

The main limitation in these studies was the use of a buffer-perfused ex vivo lung preparation that is devoid of circulating blood cells. Red blood cells may have effects on endothelial cell permeability during control, pressure, and HCA conditions that were not accounted for. These studies demonstrate that HCA can prevent pressure-induced increase in K_f but we did not assess if HCA can reverse the effect of pressure on whole lung permeability once it has increased. Such studies are the topic of future investigations.

Conclusion

We have demonstrated that HCA does not affect pulmonary hemodynamics in a manner that could account for the observed reduction in K_f and suggests that HCA inhibits endothelial mechanotransduction. We have previously demonstrated that an acute increase in hydrostatic pressure increases K_f via a heparan sulfate-nitric oxide dependent pathway[7] and we now extend this mechanism to show that inhibition of neutral sphingomyelinase activity results in barrier protection. This places neutral sphingomyelinase between heparan sulfate proteoglycans and eNOS in the mechanotransduction pathway. Additional studies are underway to elucidate the effects of HCA on heparan sulfate proteoglycan-dependent signaling and on neutral sphingomyelinase to achieve a more detailed understanding of endothelial mechanotransduction as it relates to barrier function.

Availability of data

The datasets used and/or analyzed during the current study are available from the corresponding author on reasonable request.

Conflict of interest

The authors declare that there is no conflict of interest.

Funding

Funding for this project was from the UIC, Department of Anesthesiology.

References

1. Acute Respiratory Distress Syndrome Network, Brower RG, Matthay MA, et al. Ventilation with lower tidal volumes as compared with traditional tidal volumes for acute lung injury and the acute respiratory distress syndrome. *N Engl J Med* 2000; 342(18): 1301–1308.
2. Contreras M, Masterson C and Laffey JG. Permissive hypercapnia: what to remember. *Curr Opin Anaesthesiol* 2015; 28(1): 26–37.
3. Gates KL, Howell HA, Nair A, et al. Hypercapnia impairs lung neutrophil function and increases mortality in murine pseudomonas pneumonia. *Am J Respir Cell Mol Biol* 2013; 49(5): 821–828.
4. Horie S, Ansari B, Masterson C, et al. Hypercapnic acidosis attenuates pulmonary epithelial stretch-induced injury via inhibition of the canonical NF-kappaB pathway. *Intensive Care Med Exp* 2016; 4(1): 8.
5. Otulakowski G, Engelberts D, Gusarova GA, et al. Hypercapnia attenuates ventilator-induced lung injury via a disintegrin and metalloprotease-17. *J Physiol* 2014; 592(20): 4507–4521.
6. Masterson C, Otulakowski G and Kavanagh BP. Hypercapnia: clinical relevance and mechanisms of action. *Curr Opin Crit Care* 2015; 21(1): 7–12.
7. Dull RO, Cluff M, Kingston J, et al. Lung heparan sulfates modulate K(fc) during increased vascular pressure: evidence for glycocalyx-mediated mechanotransduction. *Am J Physiol Lung Cell Mol Physiol* 2012; 302(9): L816–828.
8. Stengl M, Ledvinova L, Chvojka J, et al. Effects of clinically relevant acute hypercapnic and metabolic acidosis on the cardiovascular system: an experimental porcine study. *Crit Care* 2013; 17(6): R303.

9. Barer GR and Shaw JW. Pulmonary vasodilator and vasoconstrictor actions of carbon dioxide. *J Physiol* 1971; 213(3): 633–645.
10. Hyde RW, Lawson WH and Forster RE. Influence of carbon dioxide on pulmonary vasculature. *J Appl Physiol* 1964; 19: 734–744.
11. Brofman JD, Leff AR, Munoz NM, et al. Sympathetic secretory response to hypercapnic acidosis in swine. *J Appl Physiol (1985)* 1990; 69(2): 710–717.
12. Czarny M and Schnitzer JE. Neutral sphingomyelinase inhibitor scyphostatin prevents and ceramide mimics mechanotransduction in vascular endothelium. *Am J Physiol Heart Circ Physiol* 2004; 287(3): H1344–1352.
13. Czarny M, Liu J, Oh P, et al. Transient mechanoactivation of neutral sphingomyelinase in caveolae to generate ceramide. *J Biol Chem* 2003; 278: 4424–4430.
14. Dull RO, Mecham I and McJames S. Heparan sulfates mediate pressure-induced increase in lung endothelial hydraulic conductivity via nitric oxide/reactive oxygen species. *Am J Physiol Lung Cell Mol Physiol* 2007; 292(6): L1452–1458.
15. Hu G, Schwartz DE, Shajahan AN, et al. Isoflurane, but not sevoflurane, increases transendothelial albumin permeability in the isolated rat lung: role for enhanced phosphorylation of caveolin-1. *Anesthesiology* 2006; 104(4): 777–785.
16. Parker JC and Yoshikawa S. Vascular segmental permeabilities at high peak inflation pressure in isolated rat lungs. *Am J Physiol Lung Cell Mol Physiol* 2002; 283(6): L1203–1209.
17. Parker JC and Ivey CL. Isoproterenol attenuates high vascular pressure-induced permeability increases in isolated rat lungs. *J Appl Physiol (1985)* 1997; 83(6): 1962–1967.
18. Brower R, Wise RA, Hassapoyannes C, et al. Effect of lung inflation on lung blood volume and pulmonary venous flow. *J Appl Physiol (1985)* 1985; 58(3): 954–963.
19. Anglade D, Corboz M, Menaouar A, et al. Blood flow vs. venous pressure effects on filtration coefficient in oleic acid-injured lung. *J Appl Physiol (1985)* 1998; 84(3): 1011–1023.
20. R Foundation for Statistical Computing. *R: A language and environment for statistical computing*. Vienna: R Core Team, 2016.
21. Dowle M, Srinivasan A, Gorecki J, et al. data.table: Extension of 'data.frame'. R package version 1.10.0. 2016. Available at: https://cran.r-project.org/web/packages/data.table/index.html.
22. Dinno A. dunn.test: Dunn's Test of Multiple Comparisons Using Rank Sums. R package version 1.3.4. 2017. Available at: https://cran.r-project.org/web/packages/dunn.test/dunn.test.pdf.
23. Wickham H. *ggplot2: Elegant Graphics for Data Analysis*. New York, NY: Springer, 2009.
24. Wilke CO. cowplot: Streamlined Plot Theme and Plot Annotations for 'ggplot2'. R package version 0.7.0. 2016. Available at: https://rdrr.io/cran/cowplot.
25. Ford LE. Acute hypertensive pulmonary edema: a new paradigm. *Can J Physiol Pharmacol* 2010; 88(1): 9–13.
26. Lindsey AW, Banahan BF, Cannon RH, et al. Pulmonary blood volume of the dog and its changes in acute heart failure. *Am J Physiol* 1957; 190(1): 45–48.
27. Magder S. Volume and its relationship to cardiac output and venous return. *Crit Care* 2016; 20: 271.
28. Thorneloe KS, Cheung M, Bao W, et al. An orally active TRPV4 channel blocker prevents and resolves pulmonary edema induced by heart failure. *Sci Transl Med* 2012; 4(159): 159ra148.
29. Tzima E, Irani-Tehrani M, Kiosses WB, et al. A mechanosensory complex that mediates the endothelial cell response to fluid shear stress. *Nature* 2005; 437(7057): 426–431.
30. Siddiqui MR, Komarova YA, Vogel SM, et al. Caveolin-1-eNOS signaling promotes p190RhoGAP-A nitration and endothelial permeability. *J Cell Biol* 2011; 193(5): 841–850.
31. Guequen A, Carrasco R, Zamorano P, et al. S-nitrosylation regulates VE-cadherin phosphorylation and internalization in microvascular permeability. *Am J Physiol Heart Circ Physiol* 2016; 310(8): H1039–1044.
32. Gong H, Gao X, Feng S, et al. Evidence of a common mechanism of disassembly of adherens junctions through Galpha13 targeting of VE-cadherin. *J Exp Med* 2014; 211(3): 579–591.
33. Igarashi J, Thatte HS, Prabhakar P, et al. Calcium-independent activation of endothelial nitric oxide synthase by ceramide. *Proc Natl Acad Sci U S A* 1999; 96(22): 12583–12588.
34. Li H, Junk P, Huwiler A, et al. Dual effect of ceramide on human endothelial cells: induction of oxidative stress and transcriptional upregulation of endothelial nitric oxide synthase. *Circulation* 2002; 106(17): 2250–2256.
35. Burns AR, Zheng Z, Soubra SH, et al. Transendothelial flow inhibits neutrophil transmigration through a nitric oxide-dependent mechanism: potential role for cleft shear stress. *Am J Physiol Heart Circ Physiol* 2007; 293(5): H2904–2910.
36. Tarbell JM, Demaio L and Zaw MM. Effect of pressure on hydraulic conductivity of endothelial monolayers: role of endothelial cleft shear stress. *J Appl Physiol (1985)* 1999; 87(1): 261–268.
37. Kim MH, Harris NR and Tarbell JM. Regulation of hydraulic conductivity in response to sustained changes in pressure. *Am J Physiol Heart Circ Physiol* 2005; 289(6): H2551–2558.
38. Kim MH, Harris NR and Tarbell JM. Regulation of capillary hydraulic conductivity in response to an acute change in shear. *Am J Physiol Heart Circ Physiol* 2005; 289(5): H2126–2135.
39. DeMaio L, Tarbell JM, Scaduto RC Jr, et al. A transmural pressure gradient induces mechanical and biological adaptive responses in endothelial cells. *Am J Physiol Heart Circ Physiol* 2004; 286(2): H731–741.
40. Yin J, Hoffmann J, Kaestle SM, et al. Negative-feedback loop attenuates hydrostatic lung edema via a cGMP-dependent regulation of transient receptor potential vanilloid 4. *Circ Res* 2008; 102(8): 966–974.
41. Bellamy PE and Tierney DF. Cyclic nucleotide concentrations in tissue and perfusate of isolated rat lung. *Exp Lung Res* 1984; 7(1): 67–76.
42. Klass DJ. Lung tissue guanosine 3',5'-monophosphate: effects of ventilation and anesthesia. *J Appl Physiol Respir Environ Exerc Physiol* 1978; 45(4): 487–494.
43. Pearse DB, Wagner EM and Permutt S. Effect of ventilation on vascular permeability and cyclic nucleotide concentrations in ischemic sheep lungs. *J Appl Physiol (1985)* 1999; 86(1): 123–132.
44. Kuebler WM. The Janus-faced regulation of endothelial permeability by cyclic GMP. *Am J Physiol Lung Cell Mol Physiol* 2011; 301(2): L157–160.
45. Kuebler WM, Uhlig U, Goldmann T, et al. Stretch activates nitric oxide production in pulmonary vascular endothelial cells in situ. *Am J Respir Crit Care Med* 2003; 168(11): 1391–1398.